Structural Diversity of the Tris(di-*tert*-butylmethylsilyl)stannyl Anion: Monomeric vs Dimeric, Lithium Coordinated vs Lithium Free

Tomohide Fukawa, Masaaki Nakamoto, Vladimir Ya. Lee, and Akira Sekiguchi*

Department of Chemistry, University of Tsukuba, Tsukuba, Ibaraki 305-8571, Japan

Received January 21, 2004

The one-electron reduction of the tris(di-*tert*-butylmethylsilyl)stannyl radical (^{t}Bu$_2$MeSi)$_3$Sn$^\bullet$ was studied in a variety of solvents: polar, nonpolar, and aromatic. The structure of the resulting tris(di-*tert*-butylmethylsilyl)stannyl anion depends on the reaction conditions. Thus, the reduction of **3** with potassium in the presence of [2.2.2]cryptand resulted in the formation of the free anion **5**, whose structure is very similar to that of the THF-solvated stannyllithium species **4**. The reduction of **3** with lithium in heptane produced the dimeric structure **6**, whereas the reduction in benzene gave **7** as an anion complexed with Li(η^6-benzene). The ^{119}Sn NMR spectrum of **7** at room temperature showed a quartet at −819.8 ppm due to the ^{119}Sn−^{7}Li coupling. This gives evidence for the existence of a covalent Sn−Li bond in solution, even at room temperature.

Introduction

The anionic species of heavier group 14 elements, the heavy analogues of carbanions, are very useful synthetic groups in both organometallic and organic chemistry.[1] They can be synthesized by several methods: (i) metalation of hydrides, (ii) halogen−metal exchange, (iii) transmetalation, and (iv) reductive bond cleavage of a metal−metal bond. The chemistry of silyl and germyl anions has been greatly developed during the past decade, this activity being reflected in recent reviews on this subject.[1] In contrast, the chemistry of the tin-centered anion species has remained very poorly explored until now. Recently, we reported the synthesis of the silicon- and germanium-centered radicals **1** and **2** (Chart 1).[2] We found that these radicals can be easily reduced by alkali metals to produce stable silyl and germyl anions in more than 90% yield.[3] This very simple and rather straightforward method has some synthetic advantages: very high yield, absence of byproducts, and room-temperature conditions. Moreover, the anion structure can be affected by the reaction conditions: for example, unusual planar monomeric silyl- and germyllithiums were prepared in hydrocarbon solvents, whereas the corresponding free silyl and germyl anions were formed in THF. Quite recently, we also prepared the tin-centered radical **3** (Chart 1), a good potential precursor for the corresponding stannyl anion.[4] Here we report the one-electron reduction of this tin radical in different solvents and discuss the structural features of the resulting stannyl anion.

Chart 1

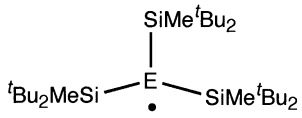

1: E = Si, **2**: Ge, **3**: Sn

Results and Discussion

1. Reduction of the Radical Tris(di-*tert*-butylmethylsilyl)stannyl (3) in a Polar Solvent. The reduction of the stannyl radical (^{t}Bu$_2$MeSi)$_3$Sn$^\bullet$ (**3**) with metallic lithium in THF produced a dark reaction mixture whose ^{119}Sn NMR spectrum showed an upfield-shifted resonance at −767.6 ppm, characteristic of stannyl anion species (Scheme 1).

The crystal structure of (^{t}Bu$_2$MeSi)$_3$SnLi(thf)$_2$ (**4**) was determined by X-ray crystallography (Figure 1). Selected bond lengths and bond angles of **4** are given in Table 1. It should be noted that very few structurally characterized examples of Lewis base coordinated stannyllithium compounds of the type R$_3$SnLi−(Lewis base) have been reported: (Me$_3$Si)$_3$SnLi(thf)$_3$,[5] Ph$_3$SnLi-

(1) Reviews: Tamao, K.; Kawachi, A. *Adv. Organomet. Chem.* **1995**, *38*, 1. (b) Lickiss, P. D.; Smith, C. M. *Coord. Chem. Rev.* **1995**, *145*, 75. (c) Belzner, J.; Dehnert, U. In *The Chemistry of Organic Silicon Compounds*; Rapport, Z., Apeloig, Y., Eds.; Wiley: New York, 1998; Chapter 14. (d) Sekiguchi, A.; Lee, V. Ya.; Nanjo, M. *Coord. Chem. Rev.* **2000**, *210*, 11. (e) Riviere, P.; Castel, A.; Riviere-Baudet, M. In *The Chemistry of Organic Germanium, Tin, and Lead Compounds*; Rappoport, Z., Ed.; Wiley: New York, 2002; Chapter 11. Recent experimental accomplishments are as follows. For silyl anions, see: (f) Lerner, H.-W.; Scholz, S.; Bolte, M. *Z. Anorg. Allg. Chem.* **2001**, *627*, 1638. (g) Jenkins, D. M.; Teng, W.; Englich, U.; Stone, D.; Ruhlandt-Senge, K. *Organometallics* **2001**, *20*, 4600. (h) Kayser, C.; Fischer, R.; Baumgartner, J.; Marschner, C. *Organometallics* **2002**, *21*, 1023. (i) Fischer, R.; Frank, D.; Gaderbauer, W.; Kayser, C.; Mechtler, C.; Baumgartner, J.; Marschner, C. *Organometallics* **2003**, *22*, 3723. For germyl anions, see: (j) Teng, W.; Ruhlandt-Senge, K. *Organometallics* **2004**, *23*, 952. For stannyl anion, see: (k) Eichler, B. E.; Power, P. P. *Inorg. Chem.* **2000**, *39*, 5444.

(2) Sekiguchi, A.; Fukawa, T.; Nakamoto, M.; Lee, V. Ya.; Ichinohe, M. *J. Am. Chem. Soc.* **2002**, *124*, 9865.

(3) Nakamoto, M.; Fukawa, T.; Lee, V. Ya.; Sekiguchi, A. *J. Am. Chem. Soc.* **2002**, *124*, 15160.

(4) Sekiguchi, A.; Fukawa, T.; Lee, V. Ya.; Nakamoto, M. *J. Am. Chem. Soc.* **2003**, *125*, 9250.

(5) Cardin, C. J.; Cardin, D. J.; Clegg, W.; Coles, S. J.; Constantine, S. P.; Rowe, J. R.; Teat, S. J. *J. Organomet. Chem.* **1999**, *573*, 96.

10.1021/om0400090 CCC: $27.50
Publication on Web 04/07/2004

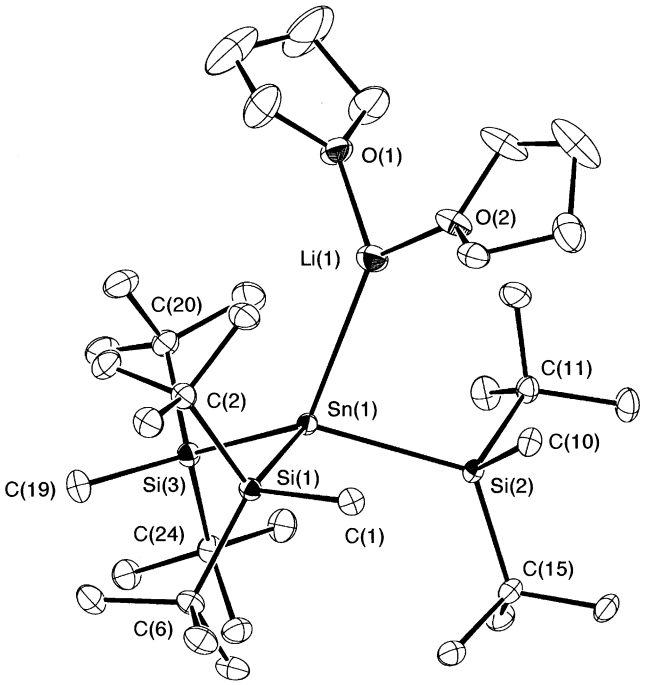

Figure 1. Molecular structure of **4** with thermal ellipsoids drawn at the 30% probability level (hydrogen atoms are omitted for clarity).

Scheme 1

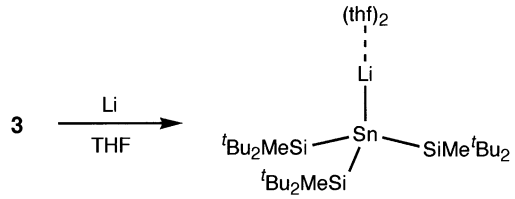

4

(pmdeta) (pmdeta = $MeN(CH_2CH_2NMe_2)_2$),[6] and $HC[Me_2SiN(p\text{-tolyl})]_3SnLi(thf)_3$.[7] The Sn−Li bond length in **4** (2.831(6) Å) is slightly shorter than the usual Sn−Li covalent bond lengths (2.86−2.89 Å).[5−7] The average Sn−Si bond length is 2.6594(7) Å, which is 0.04 Å longer than that of the corresponding radical **3** (2.6176(5) Å)[4] but still in the range of the typical Sn−Si bond length (2.561−2.789 Å).[8] It is interesting that the similar reduction of silyl and germyl radicals **1** and **2** in THF produced the corresponding silyl- and germyllithiums as solvent-separated ion pairs. Such a difference in the coordination mode among silyl-, germyl-, and stannyllithiums might be explained by the increasing size of the central anionic atom and, consequently, elongation of the distance between this central atom and the substituents ($(Si-Si)_{av}$ = 2.3617(3) Å for $(^tBu_2MeSi)_3Si^-[Li(thf)_4]^+$,[3] $(Ge-Si)_{av}$ = 2.4395(12) Å for $(^tBu_2MeSi)_3Ge^-[Li(thf)_n]^+$ (n = 3, 4),[3] $(Sn-Si)_{av}$ = 2.6594(7) Å for **4**). The long Sn−Si bonds keep the bulky substituents away from the anion center, thus leaving enough room for close contact of the lithium cation with the tin anion center. The geometry around the tin anion center is not highly pyramidalized; the sum of the Si−Sn−Si bond angles is 338.60°. This is in contrast to other stannyllithiums having highly pyramidal structures (∑(R−Sn−R) = 276.6−296.3°), including (tris(trimethylsilyl)stannyl)lithium, $(Me_3Si)_3SnLi$ (296.3°).[5] Such a tendency of **4** to planarization can be rationalized in terms of the high steric demands of the bulky Si substituents. An analogous situation was observed in $[(Me_3Si)_3Si]_3SnNa(C_7H_8)$, which has a similar pyramidalization degree (329.8°) due to the high steric requirement of bulky $(Me_3Si)_3Si$ substituents.[10b]

Table 1. Selected Bond Lengths (Å) and Bond Angles (deg) of 4 and 5[a]

	4	5
	Bond Lengths	
Sn(1)−Si(1)	2.6632(7)	2.6484(8)
Sn(1)−Si(2)	2.6672(7)	2.6509(9)
Sn(1)−Si(3)	2.6479(7)	2.6442(7)
Si(1)−C(1)	1.902(3)	1.896(3)
Si(1)−C(2)	1.951(3)	1.951(3)
Si(1)−C(6)	1.951(3)	1.951(3)
Si(2)−C(10)	1.904(3)	1.902(3)
Si(2)−C(11)	1.955(3)	1.953(3)
Si(2)−C(15)	1.944(3)	1.952(3)
Si(3)−C(19)	1.899(3)	1.893(3)
Si(3)−C(20)	1.944(3)	1.949(3)
Si(3)−C(24)	1.951(3)	1.945(3)
Sn(1)−Li(1)	2.831(6)	
	Bond Angles	
Si(1)−Sn(1)−Si(2)	109.84(2)	111.34(3)
Si(2)−Sn(1)−Si(3)	119.33(2)	111.51(3)
Si(3)−Sn(1)−Si(1)	109.45(2)	111.95(3)
Sn(1)−Si(1)−C(1)	106.34(9)	109.44(9)
Sn(1)−Si(1)−C(2)	105.94(9)	104.01(10)
Sn(1)−Si(1)−C(6)	124.46(8)	124.21(10)
Sn(1)−Si(2)−C(10)	103.11(8)	108.63(10)
Sn(1)−Si(2)−C(11)	108.71(8)	103.32(9)
Sn(1)−Si(2)−C(15)	124.37(9)	125.41(10)
Sn(1)−Si(3)−C(19)	110.54(9)	107.29(10)
Sn(1)−Si(3)−C(20)	106.90(2)	104.08(9)
Sn(1)−Si(3)−C(24)	118.31(2)	125.94(9)
Li(1)−Sn(1)−Si(1)	101.69(13)	
Li(1)−Sn(1)−Si(2)	87.66(13)	
Li(1)−Sn(1)−Si(3)	126.19(12)	

[a] Atom labeling is given in Figures 1 and 2. Standard deviations are given in parentheses.

Scheme 2

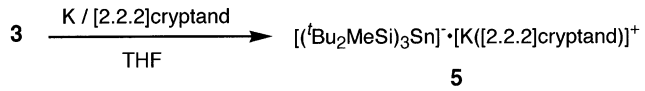

5

The free stannyl anion **5** was prepared by the reduction of **3** with potassium in THF in the presence of [2.2.2]cryptand (Scheme 2). Its crystal structure represents a free stannyl anion with a potassium cation being separated from the tin anion center by more than 7.9 Å (Figure 2; see also Table 1). Generally, anionic species of heavier group 14 elements have a highly pronounced pyramidal structure; for example, $[Ph_3Sn]^-[K([18]crown-6)]^+$ is highly pyramidalized (∑(Ph−Sn−Ph) = 290.60°).[9] However, the degree of pyramidalization around the tin anion center of anions **4** and **5** does not differ greatly (338.6 vs 334.8°). One can explain such a phenomenon

(6) Reed, D.; Stalke, D.; Wright, D. S. *Angew. Chem., Int. Ed. Engl.* **1991**, *30*, 1459.
(7) Hellmann, K. W.; Gade, L. H.; Gevert, O.; Steinert, P. *Inorg. Chem.* **1995**, *34*, 4069.
(8) Mackay, K. M. In *The Chemistry of Organic Germanium, Tin, and Lead Compounds*; Patai, S., Ed.; Wiley: New York, 1995; Chapter 2.
(9) Birchall, T.; Vetrone, J. A. *J. Chem. Soc., Chem. Commun.* **1988**, 877.
(10) For the dimeric structures $[(Me_3Si)_3SiM]_2$ (M = Li, Na, K, Rb, Cs), see: (a) Klinkhammer, K. W.; Schwarz, W. *Z. Anorg. Allg. Chem.* **1993**, *619*, 1777. (b) Klinkhammer, K. W. *Chem. Eur. J.* **1997**, *3*, 1418.

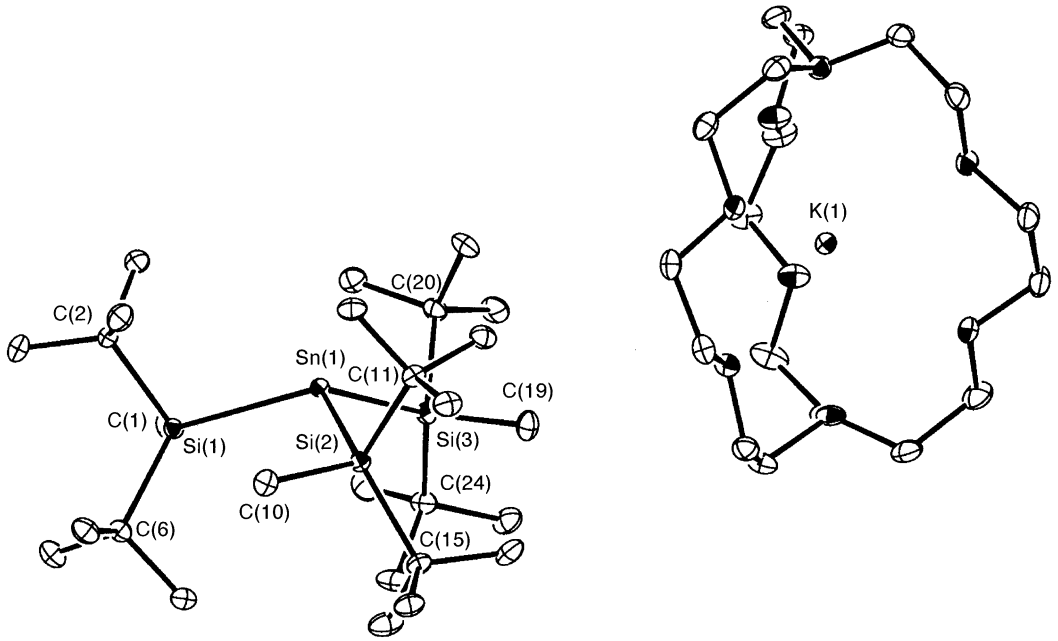

Figure 2. Molecular structure of **5** with thermal ellipsoids drawn at the 30% probability level (hydrogen atoms are omitted for clarity).

Scheme 3

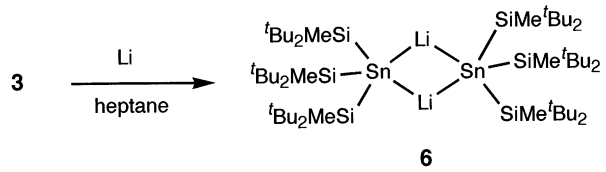

by the large steric congestion around the tin center caused by the three bulky silyl substituents, which counteract the further pyramidalization expected upon complexation of the potassium countercation with [2.2.2]-cryptand. The degree of pyramidalization of free silyl, germyl, and stannyl anions $(^tBu_2MeSi)_3E^-$ (E = Si, Ge, Sn) increases upon descending group 14 (E = Si, 349.4°;[3] E = Ge, 343.5°;[3] E = Sn, 334.8° for **5**).

2. Reduction of the Radical Tris(di-*tert*-butylmethylsilyl)stannyl (3) in a Nonpolar Solvent. The reduction of silyl and germyl radicals **1** and **2** in nonpolar solvents such as hexane and heptane produced nearly planar monomeric silyl- and germyllithiums featuring an agostic CH−Li interaction.[3] However, the reduction of **3** with Li in heptane did not result in the formation of the anticipated monomeric planar stannyllithium; the dimeric stannyllithium species $[(^tBu_2MeSi)_3SnLi]_2$ (**6**) was obtained instead (Scheme 3). The NMR spectra of **6** were impossible to obtain in hydrocarbon solvents, due to its low solubility. Dissolving **6** in aromatic or polar solvents led to the decomposition of the dimeric structure because of the unavoidable coordination of solvent molecules to the countercation.

The molecular structure of **6** was eventually determined by X-ray crystallography as a centrosymmetric rhomboid structure (Figure 3). Selected bond lengths and bond angles of **6** are listed in Table 2. The Sn−Li bond lengths are close to 3 Å (2.985(7) and 3.143(7) Å; typical Sn−Li bond length 2.86−2.89 Å).[10] The formation of a dimeric structure of **6**, in contrast to monomeric structures for $(^tBu_2MeSi)_3ELi$ (E = Si, Ge), is probably due to the less severe steric hindrance around the tin

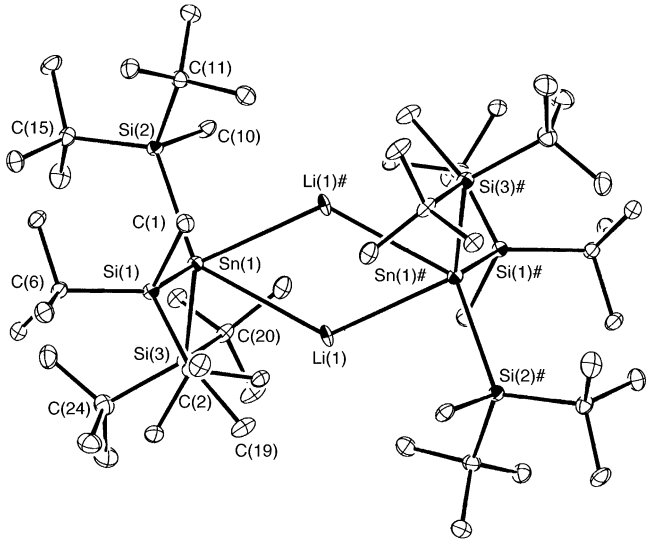

Figure 3. Molecular structure of **6** with thermal ellipsoids drawn at the 30% probability level (hydrogen atoms are omitted for clarity).

anion center in **6** allowing interaction of the two molecules to form a dimer.

3. Reduction of the Radical Tris(di-*tert*-butylmethylsilyl)stannyl (3) in an Aromatic Solvent. Reduction of **3** in benzene proceeded smoothly to form a new coordination type of stannyllithium, **7** (Scheme 4). The crystal structure of **7** was determined by X-ray crystallography (Figure 4), which showed that lithium cation in **7** is coordinated to a benzene molecule. Selected bond lengths and bond angles of **7** are given in Table 3. The lithium atom is located just below the center of the benzene ring with the $Li-C_{benzene}$ distances ranging from 2.477(5) to 2.496(5) Å. This implies an η^6 coordination mode between the lithium cation and the coordinated benzene molecule. Such π coordination of alkali-metal ions to aromatic compounds has been well studied both computationally and experimentally in the gas phase.[11] Thus, the theoretical calculations showed

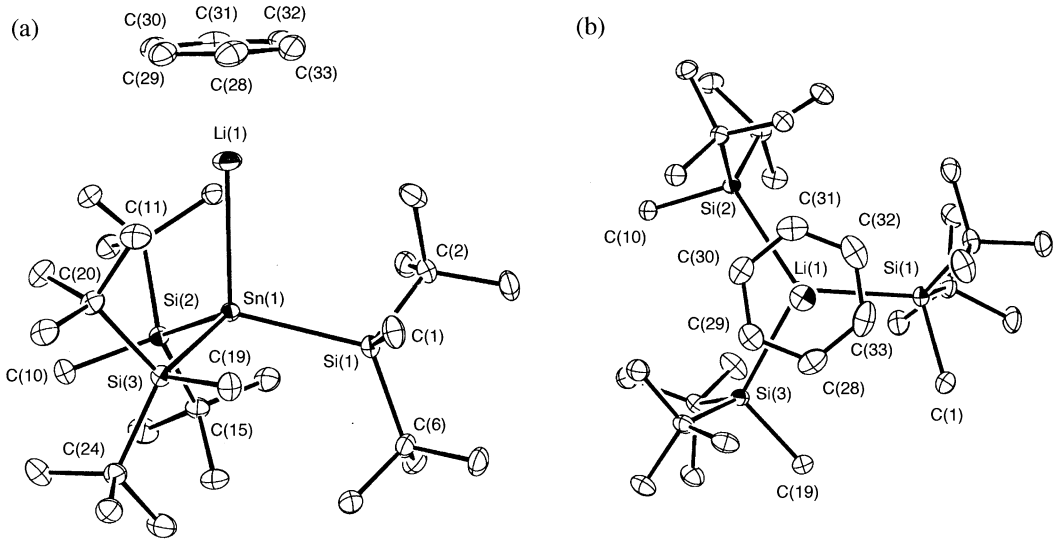

Figure 4. Molecular structure of **7** with thermal ellipsoids drawn at the 30% probability level (hydrogen atoms are omitted for clarity): (a) side view; (b) top view.

Table 2. Selected Bond Lengths (Å) and Bond Angles (deg) of 6[a]

Bond Lengths			
Sn(1)−Si(1)	2.6815(11)	Si(2)−C(11)	1.949(4)
Sn(1)−Si(2)	2.7041(10)	Si(2)−C(15)	1.947(4)
Sn(1)−Si(3)	2.6757(11)	Si(3)−C(19)	1.918(4)
Si(1)−C(1)	1.900(4)	Si(3)−C(C20)	1.945(4)
Si(1)−C(2)	1.940(4)	Si(3)−C(24)	1.937(4)
Si(1)−C(6)	1.942(4)	Sn(1)−Li(1)	3.141(7)
Si(2)−C(10)	1.904(4)	Sn(1)−Li(1)#	2.985(7)

Bond Angles			
Si(1)−Sn(1)−Si(2)	113.29(3)	Sn(1)−Si(3)−C(20)	110.36(13)
Si(2)−Sn(1)−Si(3)	112.99(3)	Sn(1)−Si(3)−C(24)	119.57(13)
Si(3)−Sn(1)−Si(1)	115.85(3)	Li(1)−Sn(1)−Si(1)	91.64(16)
Sn(1)−Si(1)−C(1)	103.27(13)	Li(1)−Sn(1)−Si(2)	138.82(14)
Sn(1)−Si(1)−C(2)	110.63(12)	Li(1)−Sn(1)−Si(3)	80.96(16)
Sn(1)−Si(1)−C(6)	121.84(12)	Li(1)−Sn(1)−Li(1)#	52.0(2)
Sn(1)−Si(2)−C(10)	106.40(11)	Li(1)#−Sn(1)−Si(1)	101.10(17)
Sn(1)−Si(2)−C(11)	109.05(12)	Li(1)#−Sn(1)−Si(2)	89.97(15)
Sn(1)−Si(2)−C(15)	120.89(12)	Li(1)#−Sn(1)−Si(3)	120.66(16)
Sn(1)−Si(3)−C(19)	104.58(13)		

[a] Atom labeling is given in Figure 3. Standard deviations are given in parentheses.

Table 3. Selected Bond Lengths (Å) and Bond Angles (deg) of 7[a]

Bond Lengths			
Sn(1)−Si(1)	2.6652(6)	Si(3)−C(C20)	1.951(2)
Sn(1)−Si(2)	2.6520(6)	Si(3)−C(24)	1.953(2)
Sn(1)−Si(3)	2.6688(6)	Sn(1)−Li(1)	2.771(4)
Si(1)−C(1)	1.902(3)	Li(1)−C(28)	2.493(5)
Si(1)−C(2)	1.950(2)	Li(1)−C(29)	2.496(5)
Si(1)−C(6)	1.943(2)	Li(1)−C(30)	2.490(5)
Si(2)−C(10)	1.888(2)	Li(1)−C(31)	2.478(5)
Si(2)−C(11)	1.948(2)	Li(1)−C(32)	2.478(5)
Si(2)−C(15)	1.933(2)	Li(1)−C(33)	2.477(5)
Si(3)−C(19)	1.900(2)		

Bond Angles			
Si(1)−Sn(1)−Si(2)	119.591(18)	Sn(1)−Si(3)−C(24)	123.30(7)
Si(2)−Sn(1)−Si(3)	110.342(17)	Li(1)−Sn(1)−Si(1)	104.11(9)
Si(3)−Sn(1)−Si(1)	108.172(18)	Li(1)−Sn(1)−Si(2)	107.88(9)
Sn(1)−Si(1)−C(1)	104.47(8)	Li(1)−Sn(1)−Si(3)	105.76(9)
Sn(1)−Si(1)−C(2)	108.72(7)	Sn(1)−Li(1)−C(28)	151.7(2)
Sn(1)−Si(1)−C(6)	122.04(7)	Sn(1)−Li(1)−C(29)	148.29(19)
Sn(1)−Si(2)−C(10)	109.80(7)	Sn(1)−Li(1)−C(30)	142.8(2)
Sn(1)−Si(2)−C(11)	107.09(7)	Sn(1)−Li(1)−C(31)	140.52(19)
Sn(1)−Si(2)−C(15)	118.55(7)	Sn(1)−Li(1)−C(32)	143.39(19)
Sn(1)−Si(3)−C(19)	107.14(7)	Sn(1)−Li(1)−C(33)	149.1(2)
Sn(1)−Si(3)−C(20)	106.24(7)		

[a] Atom labeling is given in Figure 4. Standard deviations are given in parentheses.

Scheme 4

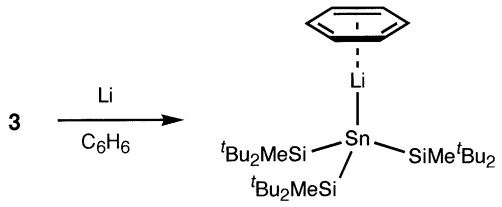

7

that the strength of the lithium−benzene π-interaction is approximately half the bonding energy of transition-metal−arene π-complexes. For example, for MeLi and PhLi, the enthalpy change upon complexation with aromatic compounds is ca. 20 kcal/mol at the MP2/6-31G** level, whereas for $Cr(C_6H_6)_2$ the Cr−benzene π-bonding energy is about 40 kcal/mol.[12] There are many examples of the crystal structures of anionic species featuring π-interactions between sodium or potassium and aromatic rings;[13] in contrast, only a few examples of similar lithium−arene π-complexes are known.[14] An η^6 type lithium−arene π-interaction has been reported only once, by Power et al. for the 2,6-bis(2,4,6-triisopropylphenyl)phenyllithium−benzene complex **8**.[15] Power's π-complex **8** and our π-complex **7** have the same π

(11) (a) Ma, J. C.; Dougherty, D. A. *Chem. Rev.* **1997**, *97*, 1303. (b) Tsuzuki, S.; Yoshida, M.; Uchimaru, T.; Mikami, M. *J. Phys. Chem. A* **2001**, *105*, 769.

(12) Tacke, M. *Eur. J. Inorg. Chem.* **1998**, 537.

(13) (a) Schaverien, C. J.; van Mechelen, J. J. *Organometallics* **1991**, *10*, 1704. (b) Fuentes, G. R.; Coan, P. S.; Streib, W. E.; Caulton, K. G. *Polyhedron* **1991**, *10*, 2371. (c) Hitchcock, P. B.; Lappert, M. F.; Lawless, G. A.; Royo, B. *J. Chem. Soc., Chem. Commun.* **1993**, 554. (d) Pu, L.; Senge, M. O.; Olmstead, M. M.; Power, P. P. *J. Am. Chem. Soc.* **1998**, *120*, 12682.

(14) (a) Pilz, M.; Allwhon, J.; Willershausen, P.; Massa, W.; Berndt, A. *Angew. Chem., Int. Ed. Engl.* **1990**, *29*, 1030. (b) Chen, H.; Bartlett, R. A.; Dias, H. V. R.; Olmstead, M. M.; Power, P. P. *Inorg. Chem.* **1991**, *30*, 2487. (c) Sekiguchi, A.; Nanjo, M.; Kabuto, C.; Sakurai, H. *Angew. Chem., Int. Ed. Engl.* **1997**, *36*, 113.

(15) Schiemenz, B.; Power, P. P. *Angew. Chem., Int. Ed. Engl.* **1996**, *35*, 2150.

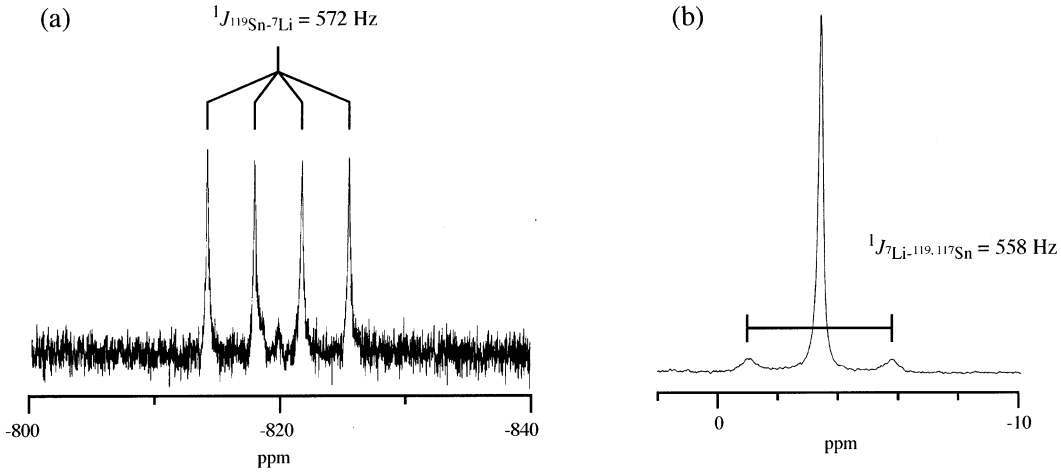

Figure 5. ^{119}Sn (a) and ^{7}Li NMR spectra (b) of **7** in C_6D_6 solution at room temperature.

Table 4. Crystallographic Data and Experimental Parameters for Crystal Structure Analysis of 4−7

	4	**5**	**6**	**7**
empirical formula	$C_{35}H_{79}LiO_2Si_3Sn$	$C_{47}H_{103}KN_2O_7Si_3Sn$	$C_{27}H_{63}LiSi_3Sn$	$C_{42}H_{78}LiSi_3Sn$
formula mass (g mol^{-1})	741.88	1050.37	597.67	792.94
collection temp (K)	120	120	120	120
λ(Mo Kα) (Å)	0.71070	0.71070	0.71070	0.71070
cryst syst	orthorhombic	orthorhombic	triclinic	monoclinic
space group	$P2_12_12_1$	*Pbcn*	$P\bar{1}$	*C*2/*c*
unit cell params				
a (Å)	14.8830(2)	16.5110(3)	11.8330(10)	38.7480(11)
b (Å)	17.0740(3)	22.4280(10)	11.7670(5)	11.8320(3)
c (Å)	17.0870(3)	31.9540(12)	15.2610(14)	24.9760(5)
α (deg)	90	90	68.863(5)	90
β (deg)	90	90	88.807(4)	125.275(1)
γ (deg)	90	90	60.453(4)	90
V (Å^3)	4342.02(12)	11832.8(7)	1691.6(2)	9348.2(4)
Z	4	8	2	8
D_{calcd} (g cm^{-3})	1.135	1.179	1.173	1.127
μ (mm^{-1})	0.696	0.606	0.874	0.648
F(000)	1600	4528	640	3400
cryst dimens (mm)	0.40 × 0.30 × 0.20	0.25 × 0.20 × 0.10	0.10 × 0.10 × 0.05	0.50 × 0.50 × 0.40
θ range (deg)	2.17−27.89	2.22−27.90	2.06−27.93	2.16−27.93
index ranges	$0 \le h \le 19$	$0 \le h \le 19$	$0 \le h \le 15$	$0 \le h \le 50$
	$0 \le k \le 22$	$0 \le k \le 29$	$-12 \le k \le 15$	$0 \le k \le 15$
	$0 \le l \le 22$	$0 \le l \le 41$	$-20 \le l \le 20$	$-32 \le l \le 26$
no. of rflns	42 656	102 416	16 823	45 774
no. of indep rflns	5690	12 783	7535	11 145
R_{int}	0.021	0.089	0.049	0.034
no. of rflns used	5690	12 783	7535	11 145
no. of params	380	547	290	425
S^a	1.083	0.901	0.943	1.006
weight parames a/b^b	0.0513/1.2162	0.0506/0.0000	0.0499/0.0000	0.0553/6.2066
R1^c ($I > 2\sigma(I)$)	0.0277	0.0399	0.0436	0.0331
wR2^d (all data)	0.0734	0.0965	0.1083	0.0887
max/min residual electron density (e Å^{-3})	1.380/−0.694	0.832/−0.778	0.991/−1.100	0.895/−0.824

^{a} $S = \{\sum[w(F_o^2 - F_c^2)^2]/(n-p)\}^{0.5}$; n = number of reflections; p = number of parameters. ^{b} $w = 1/[\sigma^2(F_o^2) + (aP)^2 + bP]$, with $P = (F_o^2 + 2F_c^2)/3$. ^{c} $R1 = \sum||F_o| - |F_c||/\sum|F_o|$. ^{d} $wR2 = \{\sum[w(F_o^2 - F_c^2)^2]/\sum[w(F_o^2)^2]\}^{0.5}$.

coordination style, but the Li−$C_{benzene}$ bond lengths of **8** (2.33(2)−2.36(2) Å) are ca. 0.15 Å shorter than those of **7** (2.477(5)−2.496 (5) Å). The reason for such a difference in Li−$C_{benzene}$ bond lengths of **7** and **8** may be the nature of the central anionic atom: a "hard" carbanion vs a "soft" stannyl anion, which causes a stronger Li−benzene π-interaction in the case of the carbanion.

The resonance of the anionic tin atom was observed at room temperature as a quartet at −819.8 ppm with the ^{119}Sn−^{7}Li coupling constant being 572 Hz. Such a splitting implies that the covalent Sn−Li bond exists in solution even at room temperature (Figure 5). In the ^{7}Li NMR spectrum of **7**, the ^{119,117}Sn satellite signals were observed with nearly the same coupling constant ($^1J_{^7Li-^{119,117}Sn}$ = 558 Hz). The nature of the Sn−Li bonding in solution has been previously studied for Ph_3-SnLi(pmdeta)[6] and $(Me_3Si)_3SnLi(thf)_3$.[5] However, no splitting was observed in both ^{119}Sn and ^{7}Li NMR at room temperature; for Ph_3SnLi(pmdeta) such a coupling was found only at −90 °C (^1J = 412 Hz).[6,16] The η^6 type lithium−arene π-interaction in **7** in solution is also demonstrated by the ^{7}Li NMR signal appearing at −3.4 ppm, which is largely shifted upfield due to the shielding

(16) The quartet splitting of the ^{119}Sn NMR resonance of the stannyl anion center due to the coupling with ^{7}Li ($^1J_{^7Li-^{119}Sn}$ = 740 Hz) was previously observed in 2,6-$Tip_2H_3C_6(Me)_2Sn$−Sn(Li)C_6H_3-2,6-Tip_2 (Tip = 2,4,6-i-Pr_3−C_6H_2).[1k]

effect of the benzene ring, whereas the ^{7}Li NMR signal of **4** can be seen at −0.57 ppm due to the lack of such an interaction.

Conclusions

We have presented here the one-electron reduction of stannyl radical with lithium and potassium in various solvents. The resulting stannyl anion has different structural features, depending on the solvent used: THF-solvated stannyllithium **4** in THF, the free anion **5** in THF in the presence of [2.2.2]cryptand, the dimeric stannyllithium **6** in heptane, and the benzene-solvated stannyllithium **7** in benzene. The structures of all compounds were elucidated by X-ray crystallography.

Experimental Section

General Procedures. All reactions involving air-sensitive compounds were carried out using a high-vacuum-line technique and dry, oxygen-free solvents. The starting material, (^{t}Bu$_2$MeSi)$_3$Sn$^{\bullet}$ (**3**), was synthesized by a previously reported method.[4] NMR spectra were recorded on Bruker AC-300FT (^{1}H NMR at 300.1 MHz; ^{13}C NMR at 75.5 MHz; ^{29}Si NMR at 59.6 MHz; ^{119}Sn NMR at 111.9 MHz; ^{7}Li NMR at 116.6 MHz) and Bruker ARX-400FT NMR spectrometers (^{1}H NMR at 400.2 MHz; ^{13}C NMR at 100.7 MHz; ^{29}Si NMR at 79.5 MHz; ^{119}Sn NMR at 149.3 MHz).

Synthesis of (^{t}Bu$_2$MeSi)$_3$SnLi(thf)$_2$ (4). Dry THF (1 mL) was transferred to a mixture of **3** (28 mg, 0.047 mmol) and Li (8 mg, 1.15 mmol). The reaction mixture was stirred overnight at room temperature to produce a clear brownish orange solution. After removal of the remaining lithium, NMR showed almost quantitative formation of **4**; yield >90%. ^{1}H NMR (THF-d_8, δ): 0.19 (s, 9 H), 1.10 (s, 54 H). ^{13}C NMR (THF-d_8, δ): 1.6, 23.4, 32.1. ^{29}Si NMR (THF-d_8, δ): 19.2. ^{119}Sn NMR (THF-d_8, δ): −767.6. ^{7}Li NMR (THF-d_8, δ): −0.57.

Synthesis of [(^{t}Bu$_2$MeSi)$_3$Sn]$^{-}$[K[2.2.2]cryptand]$^{+}$ (5). The stannyl radical **3** (20 mg, 0.034 mmol) was reduced with an excess amount of potassium (5 mg, 0.13 mmol) in the presence of [2.2.2]cryptand (13 mg, 0.035 mmol) in THF. The reaction mixture was stirred overnight at room temperature to produce a brownish orange solution. NMR measurement after removal of the excess potassium showed clean formation of **5**; yield >90%. ^{1}H NMR (THF-d_8, δ): 0.20 (s, 9 H), 1.11 (s, 54 H), 2.58 (t, J = 4.6 Hz, 12 H), 3.57 (t, J = 4.6 Hz, 12 H), 3.62 (s, 12 H). ^{13}C NMR (THF-d_8, δ): 1.7, 23.4, 32.2, 54.9, 68.5, 71.3. ^{29}Si NMR (THF-d_8, δ): 19.1. ^{119}Sn NMR (THF-d_8, δ): −765.5.

Synthesis of [(^{t}Bu$_2$MeSi)$_3$SnLi]$_2$ (6). Dry heptane (2 mL) was vacuum-transferred to a mixture of **3** (20 mg, 0.034 mmol) and Li (8 mg, 1.15 mmol), and then the reaction mixture was stirred overnight at room temperature. Excess lithium was removed by decantation, and the target compound was recrystallized from heptane.

Synthesis of (^{t}Bu$_2$MeSi)$_3$SnLi(benzene) (7). Dry benzene (0.5 mL) was transferred to a mixture of **3** (40 mg, 0.068 mmol) and Li (12 mg, 1.73 mmol). The reaction mixture was stirred overnight at room temperature to produce a clear brown solution. After removal of the remaining lithium, NMR showed formation of **7**; yield 85%. ^{1}H NMR (C_6D_6, δ): 0.47 (s, 9 H), 1.26 (s, 54 H). ^{13}C NMR (C_6D_6, δ): 1.6, 22.8, 31.8. ^{29}Si NMR (C_6D_6, δ): 24.0. ^{119}Sn NMR (C_6D_6, δ): −819.8 (q, $^{1}J_{Sn-Li}$ = 572 Hz). ^{7}Li NMR (C_6D_6, δ): −3.4.

X-ray Crystal Structure Analyses. Single crystals suitable for an X-ray diffraction study were grown from the following solvents: **4**, hexane/toluene; **5**, pentane/THF; **6**, heptane; **7**, benzene. Diffraction data were collected on a Mac Science DIP2030K image plate diffractometer employing graphite-monochromated Mo Kα radiation (λ = 0.710 70 Å). The structures were solved by direct methods and refined by full-matrix least-squares methods using the SHELXL-97 program. The crystallographic data are given in Table 4.

Acknowledgment. This work was supported by a Grant-in-Aid for Scientific Research (Nos. 13440185, 14044015, and 14078204) from the Ministry of Education, Science and Culture of Japan, the JSPS Research Fellowship for Young Scientists (T.F.), TARA (Tsukuba Advanced Research Alliance), and the COE (Center of Excellence) program.

Supporting Information Available: Tables giving details of the X-ray structure determination, fractional atomic coordinates, anisotropic thermal parameters, and bond lengths and bond angles and figures giving thermal ellipsoid plots for **4**−**7**; these data are also available as CIF files. This material is available free of charge via the Internet at http://pubs.acs.org.

OM0400090